Space Vector Modulation For Three Phase Induction Dielectric Heating

Y B Shukla and S K Joshi
Department of Electrical Engineering
The M.S.University of Baroda
Vadodara, India,
e-mail : ybshukla2003@yahoo.com, skjoshi@ieee.org

Abstract— **Modulation techniques have been widely used in induction heating, induction melting and motor drives applications. This is due to several advantages such as relatively small size of power electronics switches like MOSFET, IGBT, etc., low losses, and low cost. In this paper design and implementation of a 3-phase pulse width modulation for three phase induction dielectric heating has been described. The system has been used to control temperature using symmetrical space vector modulation. This paper presents the effect on temperature of frequency. The mathematical model has been developed and simulation on Matlab.**

Index Terms— **Induction Dielectric Heating(IDH), Space Vector modulation(SVM), Three phase inverter**

I. INTRODUCTION

THe overall performance and the cost of the heating system will be one of the important issues to be considered during the design process for the next generation of Induction Dielectric Heating (IDH) applications. The power conversion circuit (Three phase Pulse Width Modulation (PWM) inverter) of IDH applications must achieve high efficiency, low harmonic distortion, high reliability and low electromagnetic interference (EMI) noise. Three phase PWM inverter are becoming more and more popular in present day induction heating system.[17], [19], [21].

Sinusoidal Pulse Width Modulation (SPWM) has been used to control the three phase inverter output voltage. To maintains a good performance of the drive the operation has been restricted between 0 to 78 % of the value that would be reached by square wave operation. [3],[7],[17].

The various modulation strategies have been developed [3],[4],[5],[9],[10],[12],[11],[13],[17],[20],[19],[22], and analyzed. The space vector modulation (SVM) [2],[18] has been offers significant flexibility to optimize switching waveforms and it has been well suited for digital implementation.

For the IDH application, full utilization of the DC bus voltage is extremely important to achieve the maximum temperature under all conditions. The current ripple in three phase pulse width modulation inverter under steady state operation can be minimized using SVM compared to any other PWM methods for voltage control mode.

A symmetrical space vector modulation pattern has been proposed, to reduce Total Harmonic Distortion (THD) without increasing the switching losses. The design and implementations a 3-phase PWM inverter for 3-phase IDH to control temperature using space vector modulation(SVM) has been described.

II. PRINCIPLE OF SPACE VECTOR PWM

The circuit model of a typical three-phase voltage source PWM inverter is shown in Figure 1. S_1 to S_6 are the six power switches that shape the output voltage, which are controlled by the switching variables a, $a^{'}$, b, $b^{'}$ and c, $c^{'}$. When an upper MOSFET is switched on, i.e., when a, b or c is 1, the corresponding lower MOSFET is switched off, i.e., the corresponding $a^{'}$, $b^{'}$ or $c^{'}$ is 0. Therefore, the on and off states of the upper MOSFET S_1, S_3 and S_5 can be used to determine the output voltage [15].

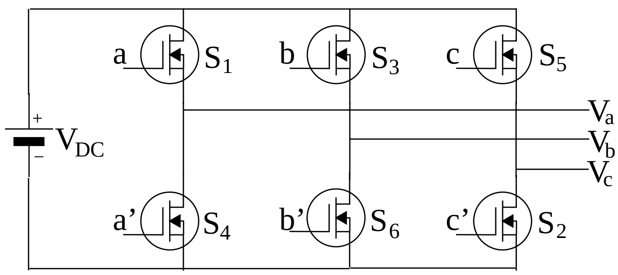

Fig. 1. 3 Phase PWM inverter circuit for IDH

The relationship between the switching variable vector $[a, b, c]^t$ and the line-to-line voltage vector $[V_{ab}, V_{bc}, V_{ca}]^t$ is given by eq. 1 in the following:

$$\begin{bmatrix} V_{ab} \\ V_{bc} \\ V_{ca} \end{bmatrix} = V_{DC} \begin{bmatrix} 1 & -1 & 0 \\ 0 & 1 & -1 \\ -1 & 0 & -1 \end{bmatrix} \begin{bmatrix} a \\ b \\ c \end{bmatrix} \quad (1)$$

Also, the relationship between the switching variable vector $[a, b, c]^t$ and the phase voltage vector $[V_{an}, V_{bn}, V_{cn}]^t$ can be expressed below.

$$\begin{bmatrix} V_{an} \\ V_{bn} \\ V_{cn} \end{bmatrix} = \frac{V_{DC}}{3} \begin{bmatrix} 2 & -1 & -1 \\ -1 & 2 & -1 \\ -1 & -1 & 2 \end{bmatrix} \begin{bmatrix} a \\ b \\ c \end{bmatrix} \quad (2)$$

As illustrated in Figure 1, there are eight possible combinations of on and off patterns for the three upper power switches. The on and off states of the lower power devices are opposite to the upper one and so are easily determined once the states of the upper power MOSFET's are determined. According to eq. 1 and 2, the eight switching vectors, output line to neutral voltage (phase voltage), and output line-to-line voltages in terms of DC-link Vdc, are given in Table I and

TABLE I

SWITCHING VECTORS, PHASE VOLTAGES AND OUTPUT LINE TO LINE VOLTAGE

Voltage Vectors	Switching Vector						Line to line voltage			Vector
	a	b	c	a’	b’	c’	V_{ab}	V_{bc}	V_{ca}	
V_0(000)	OFF	OFF	OFF	ON	ON	ON	0	0	0	Zero
V_1(100)	ON	OFF	OFF	OFF	ON	ON	V_{DC}	0	-V_{DC}	Active
V_2(110)	ON	ON	OFF	OFF	OFF	ON	0	V_{DC}	-V_{DC}	Active
V_3(010)	OFF	ON	OFF	ON	OFF	ON	-V_{DC}	V_{DC}	0	Active
V_4(011)	OFF	ON	ON	ON	OFF	OFF	-V_{DC}	0	V_{DC}	Active
V_5(001)	OFF	OFF	ON	ON	ON	OFF	0	-V_{DC}	V_{DC}	Active
V_6(101)	ON	OFF	ON	OFF	ON	OFF	V_{DC}	-V_{DC}	0	Active
V_7(111)	ON	ON	ON	OFF	OFF	OFF	0	0	0	Zero

Figure 2 shows the eight inverter voltage vectors [9] (V_0 to V_7).

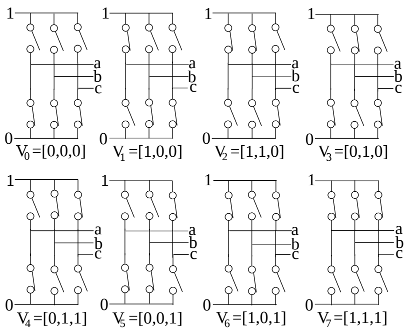

Fig. 2. Eight inverter voltage vectors

Space Vector Modulation (SVM) refers to a special switching sequence of the upper three power MOSFETs of a three-phase inverter. The source voltage has been utilized most efficiently by the space vector modulation (SVM) compared to sinusoidal pulse width modulation [9] as shown in Figure 3 .

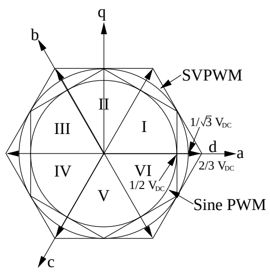

Fig. 3. Locus comparison of maximum linear control voltage in sine PWM and SVPWM.

In the vector space, according to the equivalence principle, the following operating rules are obtained:

$$V_1 = -V_4, V_2 = -V_5, V_3 = -V_6$$
$$V_0 = V_7 = 0, V_1 + V_3 + V_5 = 0 \tag{3}$$

In one sampling interval, the output voltage vector V_t can be written as

$$V_t = \frac{t_0}{T_s}V_0 + \frac{t_1}{T_s}V_1 + ... + \frac{t_7}{T_s}V_7 \tag{4}$$

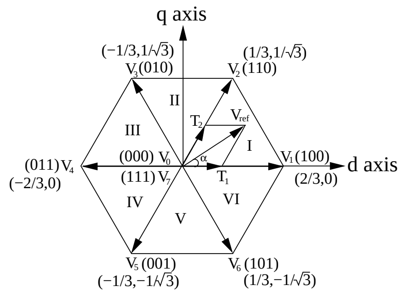

Fig. 4. The relationship of abc reference frame and stationary dq reference frame.

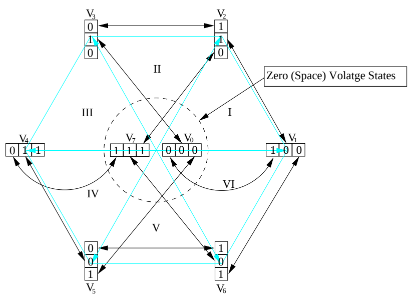

Fig. 5. Transitions between different switching states.

where $t_0, t_1, ...t_7$ are the turn-on time of the vectors $V_0, V_1, ...V_7$; $t_0, t_1, ...t_7 > 0$, $\sum_{i=0}^{7} t_i = T_s$; T_s is the sampling time.

According to eq. 3 and 4,there are infinite ways of decomposition of V into V_1, V_2, ..., V_6. However, in order to reduce the number of switching actions and make full use of active turn-on time for space vectors, the vector V is commonly split into the two nearest adjacent voltage vectors and zero vectors V_0 and V_7 in an arbitrary sector. For example, in sector I, in one sampling interval, vector V can be expressed as

$$V = \frac{T_1}{T_s}V_1 + \frac{T_2}{T_s}V_2 + \frac{T_0}{T_s}V_0 + \frac{T_7}{T_s}V_7 \tag{5}$$

where $T_s - T_1 - T_2 = T_0 + T_7 \geq 0$, $T_0 \geq 0$ and $T_7 \geq 0$.

Let the length of V be mV_{DC},where m is modulation index, then

$$\frac{m}{sin\frac{2\pi}{3}} = \frac{T_1}{T_s}\frac{1}{sin(\frac{\pi}{3} - \alpha)} = \frac{T_2}{T_s}\frac{1}{sin\alpha} \tag{6}$$

TABLE II

SPACE VECTOR MODULATION ALGORITHM

Sector I ($0 \le \omega t \le \frac{\pi}{3}$)	Sector II ($\frac{\pi}{3} \le \omega t \le \frac{2\pi}{3}$)
$T_1 = \frac{\sqrt{3}}{2} T_c m \cos(\omega t + \frac{\pi}{6})$ $T_2 = \frac{\sqrt{3}}{2} T_c m \cos(\omega t + \frac{3\pi}{2})$ $T_0 + T_7 = T_c - T_1 - T_2$	$T_2 = \frac{\sqrt{3}}{2} T_c m \cos(\omega t + \frac{11\pi}{6})$ $T_3 = \frac{\sqrt{3}}{2} T_c m \cos(\omega t + \frac{7\pi}{6})$ $T_0 + T_7 = T_c - T_2 - T_3$
Sector III ($\frac{2\pi}{3} \le \omega t \le \pi$)	Sector IV ($\pi \le \omega t \le \frac{4\pi}{3}$)
$T_3 = \frac{\sqrt{3}}{2} T_c m \cos(\omega t + \frac{3\pi}{2})$ $T_4 = \frac{\sqrt{3}}{2} T_c m \cos(\omega t + \frac{5\pi}{6})$ $T_0 + T_7 = T_c - T_3 - T_4$	$T_4 = \frac{\sqrt{3}}{2} T_c m \cos(\omega t + \frac{7\pi}{6})$ $T_5 = \frac{\sqrt{3}}{2} T_c m \cos(\omega t + \frac{\pi}{2})$ $T_0 + T_7 = T_c - T_4 - T_5$
Sector V ($\frac{4\pi}{3} \le \omega t \le \frac{5\pi}{3}$)	Sector VI ($\frac{5\pi}{3} \le \omega t \le 2\pi$)
$T_5 = \frac{\sqrt{3}}{2} T_c m \cos(\omega t + \frac{5\pi}{6})$ $T_6 = \frac{\sqrt{3}}{2} T_c m \cos(\omega t + \frac{\pi}{6})$ $T_0 + T_7 = T_c - T_5 - T_6$	$T_6 = \frac{\sqrt{3}}{2} T_c m \cos(\omega t + \frac{\pi}{2})$ $T_1 = \frac{\sqrt{3}}{2} T_c m \cos(\omega t + 11\frac{\pi}{6})$ $T_0 + T_7 = T_c - T_6 - T_1$

Thus,

$$\begin{aligned} \frac{T_1}{T_s} &= \frac{2}{\sqrt{3}} msin(\frac{\pi}{3} - \omega t) = \frac{2}{\sqrt{3}} mcos(\frac{\pi}{6} + \omega t) \\ \frac{T_2}{T_s} &= \frac{2}{\sqrt{3}} msin\omega t = \frac{2}{\sqrt{3}} mcos(\frac{3\pi}{2} + \omega t) \\ T_0 + T_7 &= T_s - T_1 - T_2 \end{aligned} \tag{7}$$

where $2n\pi \le \omega t = \alpha \le 2n\pi + \pi/3$.

The length and angle have been determine by active and zero (space) vectors. Where $V_1, V_2, ..., V_6$ are called as active vectors, and V_0, V_7 are called zero (space) vectors. The decomposition of voltage V in different sectors has been presented in Table II. Equations 5 and 6 have been commonly used for formulation of the space vector modulation. It has been shown that the turn on times $T_i(i = 1, ..., 6)$ for active vectors are identical in different space vector modulation[17],[20],[19],[22]. The different distribution of T_0 and T_7 for zero vectors yields different space vector modulation.

There are not separate modulation signals in each of the three space vector modulation technique [6]. Instead, a voltage vector is processed as a whole [1]. For space vector modulation, the boundary condition for sector I is:

$$T_s = T_1 + T_2, T_0 = T_7 = 0 \tag{8}$$

From eq. 6 to 8;

$$\frac{m}{1} = \frac{sin\frac{\pi}{3}}{sin(\frac{2\pi}{3} - \alpha)} \tag{9}$$

The boundary of the linear modulation range is the hexagon [6], [8] as shown in Figure 3. The linear modulation range is located within the hexagon. If the voltage vector V exceeds the hexagon, as calculated from eq. 7,then $T_1 + T_2 > T_s$ and it is unrealizable. Thus, for the over modulation region space vector modulation is outside the hexagon. In six step mode, the switching sequence is $V_1 - V_2 - V_3 - V_4 - V_5 - V_6$...[6]. Furthermore, it should be point out that the trajectory of voltage vector V should be circular while maintaining sinusoidal output line-to-line voltages. From Figure 4,it has been seen that for linear modulation range, the length of vector mV_{DC} should be $V = (\sqrt{3}/2)V_{DC}$, the trajectory of V becomes the inscribed circle of the hexagon and the maximum amplitude of sinusoidal line-to-line voltages is the source voltage V_{DC}.

Moreover, for space vector modulation, there is a degree of freedom in the choice of zero vectors in one switching cycle, i.e., whether V_0 and V_7 or both.

For continuous space vector schemes, in the linear modulation range, both V_0 and V_7 are used in one cycle, that is, $T_7 \ge 0$ and $T_0 \ge 0$.

For discontinuous space vector schemes, in the linear modulation range, only V_0 or only V_7 is used in one cycle, that is $T_7 = 0$ and $T_0 = 0$.

III. DESIGNING STEP FOR SVM GENERATION

To implement the space vector modulation, the voltage equations in the abc reference frame can be transformed into the stationary dq reference frame [9] as shown in Figure 6.

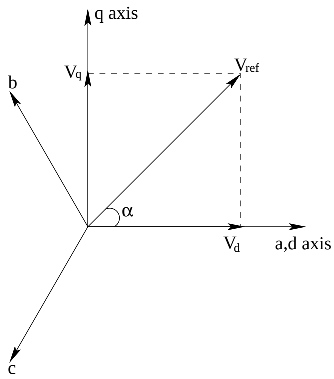

Fig. 6. Voltage Space Vector and its components in (d,q)

From Figure 6, the relation between these two reference frames is below

$$f_{dq0} = K_s f_{abc} \tag{10}$$

where, $K_s = \frac{2}{3} \begin{bmatrix} 1 & -1/2 & -1/2 \\ 0 & \sqrt{3}/2 & -\sqrt{3}/2 \\ 1/2 & 1/2 & 1/2 \end{bmatrix}$,

$f_{dq0} = [f_d, f_q, f_0]^T$, $f_{abc} = [f_a, f_b, f_c]^T$, and f denotes either a voltage or a current variable.

As described in Figure 6, this transformation is equivalent to an orthogonal projection of $[a, b, c]^t$ onto the two-dimensional perpendicular to the vector $[1, 1, 1]^t$ (the equivalent $d - q$ plane) in a three-dimensional coordinate system. As a result, six non-zero vectors and two zero vectors are possible. Six nonzero vectors (V_1 - V_6) shape the axis of a hexagonal as shown in Figure 4, and feed electric power to the load. The angle between any adjacent two non-zero vectors is 60 degrees. Meanwhile, two zero vectors (V_0 and V_7) are at the origin and apply zero voltage to the load. The eight vectors are called the basic space vectors and are denoted by V_0, V_1, V_2, V_3, V_4, V_5, V_6 and V_7. The same transformation can be applied to the desired output voltage to get the desired reference voltage vector V_{ref} in the $d-q$ plane.

The objective of space vector modulation technique is to approximate the reference voltage vector V_{ref} using the eight switching patterns.

Therefore, space vector modulation can be implemented by the following steps:

Step 1. Determine V_d, V_q, V_{ref}, and angle (α).
Step 2. Determine time duration T_1, T_2, T_0.
Step 3. Determine the switching time of each MOSFET (S_1 to S_6).

A. Determine V_d, V_q, V_{ref}, and angle (α)

From Figure 6, the V_d, V_q, V_{ref}, and angle (α) can be determine as follows:

$$\begin{aligned} V_d &= V_{an} - V_{bn}\cdot cos60 - V_{cn}\ldots cos60 \quad (11)\\ &= V_{an} - \frac{1}{2}V_{bn} - \frac{1}{2}V_{cn}\\ V_q &= 0 + V_{bn}\cdot cos30 - V_{cn}\ldots cos30\\ &= \frac{\sqrt{3}}{2}V_{bn} - \frac{\sqrt{3}}{2}V_{cn}\\ \begin{bmatrix} V_d\\ V_q\end{bmatrix} &= \frac{2}{3}\begin{bmatrix} 1 & -\frac{1}{2} & -\frac{1}{2}\\ 0 & \frac{\sqrt{3}}{2} & -\frac{\sqrt{3}}{2}\end{bmatrix}\begin{bmatrix} V_{an}\\ V_{bn}\\ V_{cn}\end{bmatrix}\\ |V_{ref}| &= \sqrt{V_d^2 + V_q^2}\\ \alpha &= tan^{-1}\left(\frac{V_d}{V_q}\right) = \omega t = 2\pi f t, \end{aligned}$$

where f = fundamental frequency

B. Determine time duration T_1, T_2, T_0

From Figure 7, the switching time duration can be calculated as follows:

• Switching time duration at sector I

$$\int_0^{T_s} V_{ref}dt = \int_0^{T_1} V_1 dt + \int_{T_1}^{T_1+T_2} V_2 dt + \int_{T_1+T_2}^{T_s} V_0 dt$$
$$T_s\cdot V_{ref} = (T_1\cdot V_1 + T_2\cdot V_2)$$

$$T_s\cdot |V_{ref}\cdot \begin{bmatrix} cos(\alpha)\\ sin(\alpha)\end{bmatrix} = T_1\cdot\frac{2}{3}\cdot V_{DC}\cdot\begin{bmatrix}1\\0\end{bmatrix} + T_2\cdot\frac{2}{3}\cdot V_{DC}\begin{bmatrix} cos(\pi/3)\\ sin(\pi/3)\end{bmatrix}$$

where, $0 > \alpha > 60^o$

$$\begin{aligned} T_1 &= T_s\cdot a\cdot\frac{sin(\pi/3-\alpha)}{sin(\pi/3)}\\ T_2 &= T_s\cdot a\cdot\frac{sin(\alpha)}{sin(\pi/3)}\\ T_0 &= T_s - (T_1 + T_2), \end{aligned}$$

where, $T_s = \frac{1}{f_s}$ and $a = \frac{|V_{ref}|}{\frac{2}{3}V_{DC}}$ • Switching time duration at any sector

$$\begin{aligned} T_1 &= \frac{\sqrt{3}\cdot T_s\cdot |V_{ref}|}{V_{DC}}\left(sin\left(\frac{\pi}{3} - \alpha + \frac{n-1}{3}\pi\right)\right)\\ &= \frac{\sqrt{3}\cdot T_s\cdot |V_{ref}|}{V_{DC}}\left(sin\frac{n}{3}\pi - \alpha\right)\\ &= \frac{\sqrt{3}\cdot T_s\cdot |V_{ref}|}{V_{DC}}\left(sin\frac{n}{3}\pi cos\alpha - cos\frac{n}{3}\pi sin\alpha\right)\\ T_2 &= \frac{\sqrt{3}\cdot T_s\cdot |V_{ref}|}{V_{DC}}\left(sin\left(\alpha - \frac{n-1}{3}\pi\right)\right)\\ &= \frac{\sqrt{3}\cdot T_s\cdot |V_{ref}|}{V_{DC}}\\ &\quad\left(-cos\alpha\cdot sin\frac{n-1}{3}\pi + sin\alpha\cdot cos30\frac{n-1}{3}\pi\right)\\ T_0 &= T_s - T_1 - T_2 \end{aligned}$$

where, n=1 through 6 (that is, Sector I to VI) $(n-1)\frac{\pi}{3} \le \alpha \le \frac{n\pi}{3}$

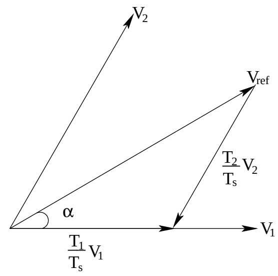

Fig. 7. Reference vector as a combination of adjacent vectors at sector I

C. Determine the switching time of each MOSFET (S_1 to S_6)

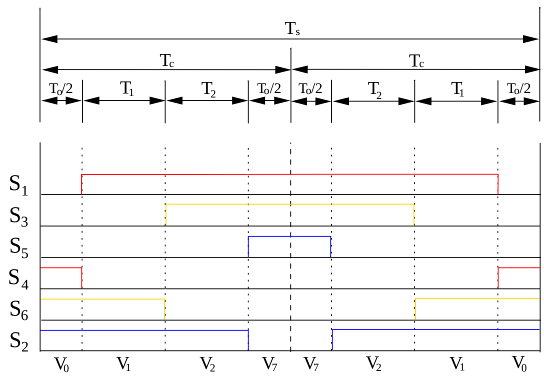

Fig. 8. Actual gating signal pattern of the space vector PWM(in the case of the sector -1

Based on Figure 8, the switching time at each sector has been summarized in Table III, and it will be built in Simulink model to implement SVM.

IV. Simulation Results

Simulation results were performed using simulink block as shown in Figure 9. The DC bus V_{DC} is equal to $325V$,

TABLE III

SWITCHING TIME CALCULATION AT EACH SECTOR

Sector	Upper Switches (S_1, S_3, S_5)	Lower Switches (S_4, S_6, S_2)
1	$S_1 = T_1 + T_2 + T_7$ $S_3 = T_2 + T_7$ $S_5 = T_7$	$S_4 = T_0$ $S_6 = T_1 + T_0$ $S_2 = T_1 + T_2 + T_0$
2	$S_1 = T_2 + T_7$ $S_3 = T_2 + T_3 + T_7$ $S_5 = T_7$	$S_4 = T_3 + T_0$ $S_6 = T_0$ $S_2 = T_2 + T_3 + T_0$
3	$S_1 = T_7$ $S_3 = T_3 + T_4 + T_7$ $S_5 = T_4 + T_7$	$S_4 = T_3 + T_4 + T_0$ $S_6 = T_0$ $S_2 = T_3 + T_0$
	$T_7 = T_o/2$	$T_0 = T_o/2$

is connected to the input of the inverter. For the linear operating range the V_{ref} must not exceeds the boundary of the hexagon. Therefore the maximum amplitude of the desired V_{ref} is calculated as

$$|V_{ref}|_{max} = \sqrt{\left(\frac{2}{3}V_{DC}\right)^2 - \left(\frac{2}{6}V_{DC}\right)^2} \qquad (12)$$

Sample circuit parameters are given in Table IV. Simulation

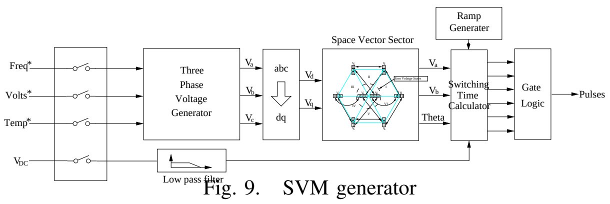

Fig. 9. SVM generator

space vector generator has been shown in Figure 9 Three phase PWM inverter output line to line voltage , output current , 3 phase to 2 phase dq transformation voltages and 3 phase to 2 phase dq transformation currents are shown in Figure 10 , 11, 12, 13 respectively. Simulation summaries and results are given in Table V, VI respectively.

A spectral analysis of all waveforms is performed and all harmonics are presented in Table VII. These results shows that acceptable performances can be obtained at all testing frequencies since the total harmonic distortion (THD) did never reach 10 % . At high switching frequency the PWM converter generate a voltage having an amplitude close to the desired value.

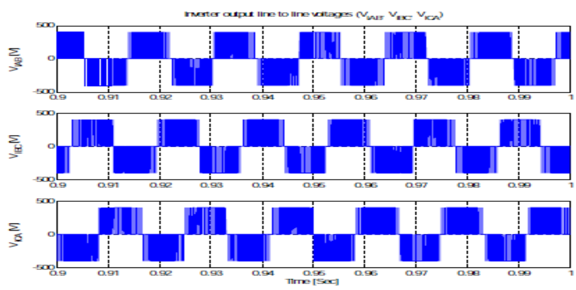

Fig. 10. Simulation results of inverter output line to line voltages $(V_{iAB}, V_{iBC}, V_{iCA})$

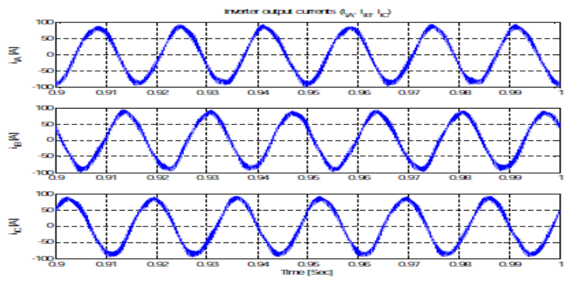

Fig. 11. Simulation results of inverter output currents (i_{iA}, i_{iB}, i_{iC})

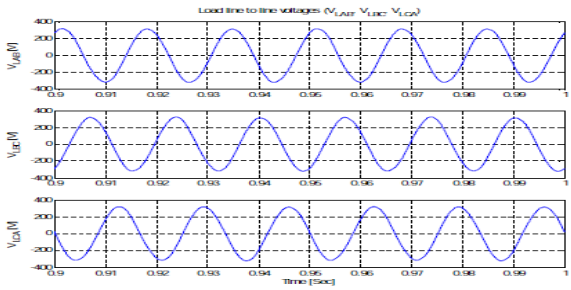

Fig. 12. Simulation results of load voltages $(V_{LAB}, V_{LBC}, V_{LCA})$

V. CONCLUSIONS

Space vector modulation only requires on reference space vector to generate three phase sine waves. The amplitude and frequency of load voltage can be varied by controlling the reference space vector. Furthermore, this algorithm is flexible and suitable for advanced vector control. The strategy of the switching minimizes the distortion of load current as well as loss due to minimize number of commutations in the inverter.

Simulation of Space Vector Modulation (SVM) technique has been done using MATLAB. This aim on the one hand to prove the effectiveness of the SVM in the contribution in the switching power losses reduction. SVM is among one of the best solution to achieve good voltage transfer and reduce harmonic distortion in the output of three phase inverter for IDH. It also provide excellent output performance optimized

TABLE IV

CIRCUIT PARAMETERS

Parameter	Value
Utility	220V/50Hz
V_{DC}	325 volt
L_m	69.31mH
f_{sw}	2Khz

TABLE V

SIMULATION RESULTS

Switching Freq. in Hz	Set Temp. in ^0C	Final Temp. in ^0C	V_{ab} in Volt	Frequency in Hz	Load current in Amp.
200	1200	1167	139.21	41.01	9.036
2000	1200	1170	153.49	41.74	6.107
20000	1200	1168	151.33	41.74	5.186
200000	1200	1190	175.95	41.74	4.765

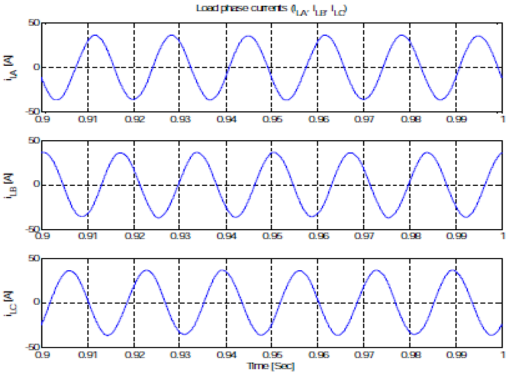

Fig. 13. Simulation results of load phase currents (i_{LA}, i_{LB}, i_{LC})

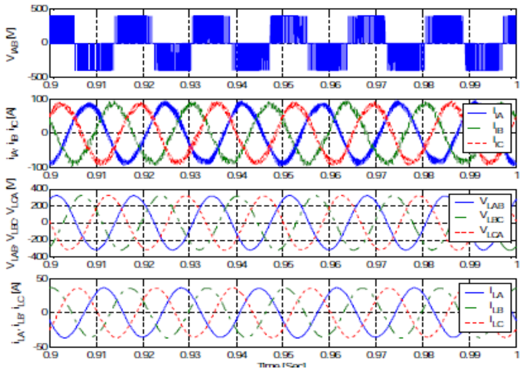

Fig. 14. Simulation waveforms. (a) Inverter output line to line voltage (V_{iAB}) (b) Inverter output current (i_{iA}) (c) Load line to line voltage (V_{LAB}) (d) Load phase current (i_{LA})

efficiency and high reliability compared to similar three phase inverter with conventional pulse width modulations.

TABLE VI

SIMULATIONS SUMMARIES

Set Temp. in ^0C	Final Temp. in ^0C	V_{ab} in Volt	Frequency in Hz
150	145.8	15.20	16.42
530	499	67.22	18.44
1300	1275	165.84	45.21
1500	1484	191.75	52.17
1200	1170	153.49	41.74

TABLE VII

SPECTRAL ANALYSIS

h	Harmonic for different Switching frequencies			
	1 kHz	3 kHz	5 kHz	10 kHz
0	-4.58	-4.58	-4.16	-4.16
1	81.22	80.83	73.33	73.24
2	3.22	2.99	2.64	2.60
3	4.70	4.53	4.06	4.03
4	0.42	0.20	0.11	0.06
5	4.45	5.04	4.80	4.94
6	1.98	1.79	1.58	1.55
7	1.03	1.07	0.99	1.00

REFERENCES

[1] Van der Broeck, Skudelny, H.C., Stanke, G., *Analysis and Realization of a Pulse Width Modulator Based on Voltage Space Vectors*, Conference Rec. Annual Meeting IEEE-IAS, Denver/USA, pp.244-251, 1986.

[2] H. Van der Broeck, H. Skudelny, and G. Stanke, *Analysis and realization of a pulse width modulator based on voltage space vectors*, in Proc. IEEE Ind. Appl. Conf., pp.244-251,1986.

[3] H.W. Van der Broek, H.C. Skudelny, and G.V. Stanke, *Analysis and realization of a pulse width modulator based on voltage space vectors*, IEEE Trans. Ind. Applicat., Vol.24, pp.142 ? 150, Jan./Feb.-1988.

[4] D.Casadei,G.Grandi,G.Serra and A Tani, *Sapce vector control of matrix converters with unity input power factor and sinusoidal input/output waveforms*, European power electronics assocation,1993.

[5] T.G.Habelter,*A sapce vector based rectifier regulator for AC/DC/AC converter*, IEEE Trans. on Power Elec.,Vol.8, No.1, pp.30-36, 1993.

[6] J. Holtz, *Pulse width modulation for electronics power conversion* , Proceedings IEEE, Vol.82, pp.1194-1214, Aug-1994.

[7] Z. Yu, A. Mohammed, and I. Panahi, *A review of three pwm techniques*, in Proc. Amer. Control Conf.,pp. 257 ? 261, 1997.

[8] D. W. Chung, J. S. Kim, and S. K. Sul, *Unified voltage modulation technique for real time three phase power conversion*, IEEE transactions industrial application , Vol.34, pp.374-380, Mar./April-1998.

[9] Do-Hyun Jang, and Duck-Yong Yoon, *Space-vector PWM techniques for two phase inverter fed two phase induction motor*, IEEE Conf., 1999.

[10] Peter Vas, *Artificial ?Intelligence based electrical machines and drives*, Oxford university, 1999.

[11] J. Klima, *Analytical model for the time and frequency domain analysis of space-vector PWM inverter fed induction motor based on the Laplace transform of space-vectors*, in Proc. Power Conversion Conf., Osaka, Japan, pp. 1334 ? 1339, 2002.

[12] G. Narayanan and V.T. Ranganathan, *Extension of operation of space vector PWM strategies with low switching frequencies using different overmodulation algorithms*, IEEE Trans. Power Electron., Vol.17, pp.788 -789, Sept.-2002.

[13] Mondal, S.K., Bose, B.K., Oleschuk, V., Pinto, J.O.P, *Space vector pulse width modulation of three-level inverter extending operation into overmodulation region*, IEEE Transactions on Power Electronics Vol.18, Issue 2, pp.604 ? 611, March-2003.

[14] Kelly, J.W. Strangas, E.G. Miller, J.M. *Multiphase Space Vector pulse width modulation*, IEEE Trans. on Energy Conservations, Vol.18, No.2, pp.254-264, June-2003.

[15] Do-Hyun Jang, and Duck-Yong Yoon, *Space-vector PWM techniques for two phase inverter fed two phase induction motor*, IEEE Trans. On industry applications, Vol.39, No.2, pp.542-549, Mar./Apr.-2003.

[16] M.A. Jabbar, Ashwin M. Khambad Kone, and Zhang Yanfeng, *Space-vector modulation in a two phase induction motor drive for constant power operation*, IEEE Trans. on Industrial Electronics, Vol.51, No.5, pp.1081-1088, Oct.-2004.

[17] S Behera, S P Das and S R Doradla, *A New SVM Technique for Soft-switched dc-ac Converter*, IE (I) Journal EL, Vol.85, March-2005.

[18] L. Franquelo, M. Prats, R. Portillo, J. Galvan, M. Perales, J. Carrasco, E. Diez, and J. Jimenez, *Three-dimensional space-vector modulation algorithm for four-leg multilevel converters using abc coordinates*, IEEE Trans. Ind. Electron., Vol.53, No.2, pp. 459-466, Apr.-2006

[19] A.Iqbal, *Analysis of space vector pulse width modulation for a five phase voltage source inverter*,IE (I)journal-EL, Vol.89 Issue 3, pp.8-15, Sep.-2008.

[20] Bosquets Monge. S, Bordonau. J., Rocabert. J, *A virtual vector pulse width modulation for a four level diode clamped DC-AC converter*, Power Electronics, IEEE Transaction, Vol.23, pp.1964 -1972, July-2008.

[21] Nabil A. Ahmed, *Three phase high frequency AC conversion circuit with dual mode PWM/PDM control strategy for high power IH application*, Proc. of world academy of science, Engineering and Technology Vol.35, Nov.-2008.

[22] R.Arumaozhiyal and K.Baskaran, *Space vector pulse width modulation based speed control of induction motor using fuzzzy PI controller*, International Journal of Computer and Electrical Engineering, Vol.1, No.1, pp. 1793-8198, April-2009.